

RSC Advances



This is an *Accepted Manuscript*, which has been through the Royal Society of Chemistry peer review process and has been accepted for publication.

Accepted Manuscripts are published online shortly after acceptance, before technical editing, formatting and proof reading. Using this free service, authors can make their results available to the community, in citable form, before we publish the edited article. This *Accepted Manuscript* will be replaced by the edited, formatted and paginated article as soon as this is available.

You can find more information about *Accepted Manuscripts* in the [Information for Authors](#).

Please note that technical editing may introduce minor changes to the text and/or graphics, which may alter content. The journal's standard [Terms & Conditions](#) and the [Ethical guidelines](#) still apply. In no event shall the Royal Society of Chemistry be held responsible for any errors or omissions in this *Accepted Manuscript* or any consequences arising from the use of any information it contains.

Cite this: DOI: 10.1039/c0xx00000x

www.rsc.org/xxxxxx

Paper

A simple and effective strategy for the directed and high-yield assembly of large-sized gold nanoparticles driven by bithiol-modified complementary dsDNA architectures

Yan-Fang Cheng,^{#bc} Gui-Ping Yu,^{#b} Yuan Yan,^b Jian-Yu Liu,^{*b} Cui Ye,^b Xiang Yu,^{*a} Xuan-Di Lai^b and Jian-Qiang Hu^{*b}

Received (in XXX, XXX) Xth XXXXXXXXX 20XX, Accepted Xth XXXXXXXXX 20XX

DOI: 10.1039/b000000x

A simple and effective strategy for the directed and high-yield assembly of large-sized Au NPs has been demonstrated by bithiol-modified complementary dsDNA architectures. The dsDNA architectures were formed by mixing two complementary thiol-modified ssDNA (only 36 bases) and played an important role in the high-yield self-assembly of the large-sized Au NPs. Compared with traditional methods, this strategy was simple, effective, low-cost and enabled excellent self-assembly of large-sized Au NPs, while obviating the conjugate of Au NPs to ssDNA and the use of long chain DNA. Therefore, this straightforward and high efficiency methodology opens a new avenue of DNA-induced self-assembly of large-sized metal NPs.

1 Introduction

DNA programmable self-assembly of metal nanostructures has been attracting tremendous attention because it offers tailored optical and electrical properties and exciting prospects of generating new functional materials.¹⁻⁵ The properties of metal nanoassemblies (NAs) are known to be closely dependent on the sizes, shapes and surface properties of metal nanoparticles (NPs), self-assembly strategy and interparticle spacing and hierarchical organization of metal NAs.⁶⁻¹⁰ Of these elements, self-assembly unit size and assembly strategy are of fundamental importance for obtaining desirable metal NAs. Currently, metal NPs of relatively small sizes (2-10 nm) have been expertly assembled by short-chain thiol-modified DNA and four steps strategy, *i.e.*, metal NPs and DNA conjugating, gel electrophoresis separation, self-assembling and the second gel electrophoresis separation.^{11,12} Generally, thiol-modified single-stranded DNA (ssDNA) molecules are first conjugated to metal NPs, and the NPs with well-defined DNA molecule numbers are separated by gel electrophoresis; then two sorts of purified DNA-NPs with complementary DNA chains begin to assemble by base pairing, the resulting NAs are finally purified for obtaining metal NAs with well-defined NPs numbers (*e.g.*, dimers and trimers) by the second gel electrophoresis. Additionally, more steps (>4 steps) are required if the self-assembly strategy involves in templates or polymers.¹³

The above-mentioned DNA self-assembly methodology is relatively complex and time-consuming. Moreover, it is only available to assemble small-sized metal NPs. If the strategy needs to be extendable for assembling large-sized metal NPs that have utility for plasmonic application, it is usually required to

link additional long DNA strands (usually more than 100 bases) for obtaining well-defined ssDNA-NPs assembly units. For example, it has been demonstrated that the 18-nm Au NPs containing different ssDNA numbers can be effectively separated only through conjugating additional long ssDNA of ≥ 100 bases.¹⁴ Busson's group also revealed that the gel electrophoresis separation of the 27 or 36 nm Au NPs coupled with different numbers of ssDNA molecules required the additional use of 400 and 500 bases DNA, respectively.¹⁵ Thus, it remains a great challenge to design a simple and effective strategy to assemble large-sized metal NPs.

In this work, we reported a straightforward and effective method for the directed and high-yield assembly of large-sized Au NPs (*ca.* 22.6 and 48.0 nm), which involved bithiol-modified complementary double-stranded DNA (dsDNA) architectures. The dsDNA architectures were formed by mixing two complementary thiol-modified ssDNA (only 36 bases). In the self-assembly strategy, it was found that dsDNA architectures and the concentration ratios of Au:dsDNA played a crucial role in the formation of Au NAs. Only when the concentration ratio of Au:dsDNA was lower than 1:20, high-yield Au NAs with well-defined Au NPs numbers could be acquired. Compared with traditional methods, this strategy was simple, effective and low-cost and enabled excellent self-assembly of large-sized Au NPs, while obviating the conjugate of Au NPs to ssDNA and the use of long chain DNA. Given this superiority, we believe that our method will provide a preferable alternative for large-sized NPs and DNA conjugating, as far as the self-assembly of other large-scale metal NPs.

2 Experimental

2.1 Reagents and materials

1×TBE buffer: tris(hydroxymethyl)aminomethane (Tris, 89 mM), boric acid (89 mM), and ethylenediaminetetraacetic acid (EDTA, 2 mM), pH 8.0. Tris, EDTA, boric acid, NaCl, Dithiothreitol (DTT), and Bis(p-sulfonatophenyl)phenylphosphine (BSPP) were obtained from Strem Chemicals. NAP-5 columns Sephadex G-25 DNA grade was purchased from GE Healthcare. DNA oligonucleotides used in this study were synthesized by Sangon Biotech and the sequences are listed as below: DNA1, 5'-HS-(CH₂)₆-ATC CTG ACA TCG GCA CGA GTA TTT CTA CCA TGT ATC-3'; cDNA1, 5'-HS-(CH₂)₆-GAT ACA TGG TAG AAA TAC TCG TGC CGA TGT CAG GAT-3'.

2.2 Synthesis of water-soluble 22.6-nm and 48.0-nm Au NPs

The Au NPs of about 22.6 nm were prepared according to the previously reported method.¹⁶ Briefly, 40 mL 2.5 × 10⁻⁴ M HAuCl₄ solution was heated to 120 °C in an oil bath under vigorous stirring for 30 min. Subsequently, 4 mL 1% Na₃C₆H₅O₇ solution was added into the above solution quickly. After continue stirring 20 min, the boiled solution turned ruby red, indicating the formation of the Au NPs in the solution. Finally, the growth of the Au NPs was quenched by cooled deionized water (4 °C).

To further investigate the bithiol-modified complementary dsDNA strategy, Au NPs with the average diameter of approximate 48.0 nm were synthesized by the seed-induced growth method. Briefly, Au seeds (ca. 16 nm) were firstly prepared according to the literature.¹⁷ 26.3 mL of the Au seed solution (2 nM) was then added by 5 mL of sodium citrate (1% w/v), 5 mL of HAuCl₄ solution (24.2 mM) and 5 mL of ascorbic acid (1% w/v) separately over 1 h. Next, the mixture was heated to boiling and kept stirring for 30 min. Finally, the 48.0-nm Au NPs were obtained through centrifuging the cooled solution 2 times at 5000 rpm for 15 min.

2.3 Phosphination and concentration of the Au NPs

Briefly, 6 mg BSPP was added into the 20 mL Au NPs solution and stirred constantly overnight at low speed to replace the citrate group capping the Au NPs and make the Au NPs have better stability and not aggregate under the salted solution.¹⁸ Then, NaCl (solid) was added slowly to the mixture until the color change was observed from burgundy to purple. The resulting mixture was centrifuged at 4000 rpm for 30 min and the supernatant was carefully removed with a pipette. The concentrated Au NPs were finally resuspended in BSPP solution (2.5 mM), in which the Au NPs concentration (ca. 0.1 μM) was quantified by assaying its absorbency at 520 nm (the extinction coefficient was estimated to about 7.2 × 10⁸ L/(mol · cm)).¹⁹

2.4 Activation of thiolated single-stranded DNA molecules

The thiol-functionalized DNA molecules were activated by the addition of 0.1 M dithiothreitol (DTT) for at least 2 h in 4 °C (typically, 2.5 OD DNA molecules need 100 μL 0.1 M DTT). The activated DNA solution was purified through using NAP-5 columns. The DNA concentrations (DNA1: 7.4 μM; cDNA1: 5.1 μM) were determined through UV-vis absorption at 260 nm.

2.5. Au NPs Self-Assemblies. First, equal molars of solutions of DNA1 and cDNA1 were mixed in a buffer solution containing 5

mg/mL BSPP and 50 mM NaCl. The mixture was incubated in a water bath at 85 °C for 10 min and cooled down slowly to room temperature overnight. Then the complementary double chain DNA molecules were mixed with AuNPs with different molar ratios (e.g., Au:DNA = 1:5, 1:10, 1:15, 1:20, 1:40 and 1:60) in 1 × TBE buffer. Finally, the self-assemblies were incubated at room temperature for 4-10 h.

2.5 Gel electrophoresis

The self-assemblies were first loaded on 3% agarose gels (1×TBE as running buffer) after adding a volume of 60% glycerol equivalent to one fifth of the self-assemblies. Then the gels were performed at 5 V/cm for 1.5 h to obtain different bands. Finally, the gel bands were cut out and immersed in ultrapure water overnight for acquiring different self-assemblies.

2.6 Instruments

Transmission electron microscopy (TEM) studies were performed by using a FEI TECNAI 10 microscope operated at 100 kV. High-resolution TEM (HRTEM) measurement was carried out by a JEOL 2100F microscope with an acceleration voltage of 200 kV. TEM grids were prepared by placing 5 μL of the as-prepared self-assemblies suspensions. After 15 min, the excess solutions were wiped off by lightly touching one edge of the grids with a filter paper. Atomic force microscopy (AFM) image was obtained through using Si-Al-coated cantilevers (BRUKER, USA) with resonance frequency of 150 kHz. The AFM sample was prepared by dropping 20 μL 2.0 nM Au nanoassemblies (dimers) into freshly prepared mica surface for 5 min and then washing with distilled water and drying by nitrogen blow. UV-visible (UV-vis) absorption spectrum was acquired with a Hewlett-Packard 8452 diode array spectrometer (U-3010).

3 Results and discussion

3.1 Intrinsic features of the dsDNA-induced self-assembly strategy

Our studies started with constructing bithiol-modified complementary dsDNA linkers by mixing equal amount of DNA1 and cDNA1. Compared with thiol-modified ssDNA, the bithiol-modified dsDNA (DNA1/cDNA1) had the following

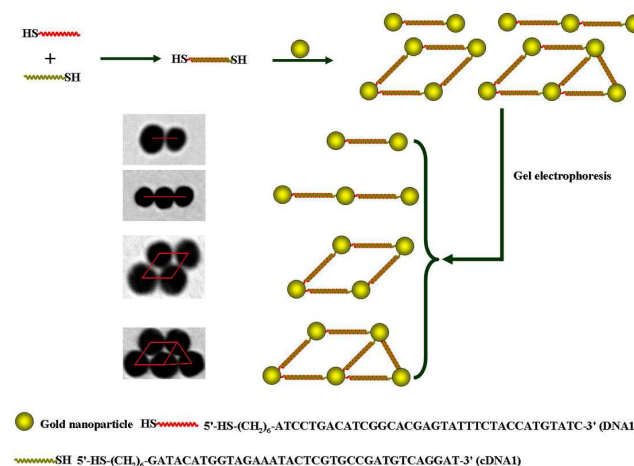


Fig. 1 Schematic representation of the large-sized Au NPs self-assembly driven by the bithiol-modified dsDNA (DNA1/cDNA1) architectures.

advantages: (i) the dsDNA had a rigid structure; (ii) the dsDNA bore two thiol groups, one at each end; (iii) the dsDNA could be utilized to directly assemble metal NPs. Thus, upon introducing Au NPs with the average size of about 22.6 nm (Fig. S1), the dsDNA linkers easily induced the self-assembly of the Au NPs (Fig. 1). Moreover, the dsDNA-Au NPs assemblies were easily separated into the Au NAs with well-defined Au NPs numbers by gel electrophoresis. Compared with previously assembling strategies of large-sized Au NPs, the dsDNA strategy used only short DNA strands (36 bases) and simplified the procedures by removing two steps, *i.e.*, the conjugation of thiol-modified ssDNA with the Au NPs and the gel electrophoresis separation to obtain Au NPs with defined ssDNA numbers.

3.2 Gel electrophoresis of the dsDNA-Au NPs conjugates

Fig. 2 shows the gel electropherogram of the dsDNA-Au NPs conjugates prepared from different stoichiometries. At relatively high Au NPs concentration (*i.e.*, the concentration ratio of Au NPs to dsDNA was 1:15 or higher), only a single band which was quite close to that of the Au NPs alone in Lane 1 could be discerned (Fig. 2, Lanes 2-4), indicating the unsuccessful assembly of the Au NPs, despite of appearing a tiny amount of Au NAs with two (*ca.* 5%) or three (*ca.* 3%) Au NPs (Fig. S2).^{11,20} Nevertheless, the observed single band tended to disperse as the dsDNA concentration increased (Lanes 2-4 of Fig. 2), which indicated the slow increase of the Au NAs quantity. When the dsDNA concentration increased or the concentration ratio of the Au NPs to dsDNA lowered to 1:20 (herein, the Au NPs concentration kept unvaried), three distinct bands were easily discerned in the gel electropherogram (Lane 5 of Fig. 2), corresponding to isolated Au NPs (bottom) and Au NAs containing two (middle) or three (top) Au NPs. This suggested that the Au NPs began to assemble at this concentration ratio, although the non-assembled Au NPs were still dominant.

Very interesting, when the concentration ratio lowered to 1:40, the isolated Au NPs completely assembled into the Au NAs containing two, three, four, five or more Au NPs (Lanes 6 and 7 of Fig. 2). Furthermore, it could be seen that the smaller NAs had higher content, probably due to their lower steric hindrance. For example, the two-Au NPs nanoassembly had the highest content (*ca.* 60%). Besides, in Fig. 2, compared with the corresponding bands in Lane 6, the first band of Lane 7 had higher intensity whereas the second, third and fourth bands had relatively weaker intensity, indicating that the low concentration ratio of Au NPs to dsDNA was not suitable for generating large NAs through the dsDNA self-assembly strategy. To illustrate the bithiol-modified

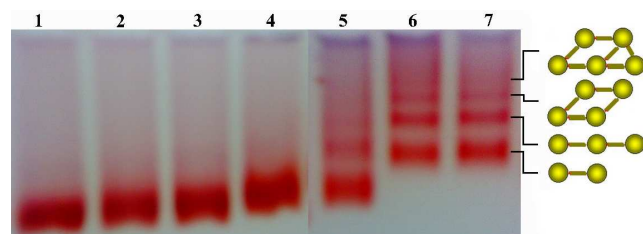


Fig. 2 Gel electropherogram of the Au NPs conjugated with different concentrations of thiolated DNA1/cDNA1. Lane 1: Au NPs alone; Lanes 2-7: the concentration ratios of the Au NPs to the dsDNA are 1:5, 1:10, 1:15, 1:20, 1:40, and 1:60, respectively. The zones with different Au NP assemblies are showed at the right side.

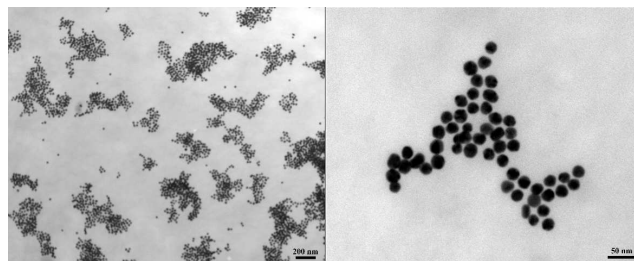


Fig. 3 (A) TEM of the large Au NAs prepared by stepwise assembly. The Au NPs were first coupled with DNA1 and cDNA1 individually (molar ratio: 1:60), and the resulting DNA1-Au NPs and cDNA1-Au NPs were then mixed to directly give the large Au NAs without gel electrophoresis separation; (B) TEM image of a representative large Au NA.

dsDNA role in the self-assembly of the large-sized Au NPs, a comparative study was performed. Coupling the Au NPs with DNA1 and cDNA1 individually and mixing the resulting DNA1-Au and cDNA1-Au conjugates without gel electrophoresis separation would give large Au NAs (Fig. 3). Moreover, the Au dimmers, trimers, tetramers and pentamers in Fig. 3 could not be partitioned by gel electrophoresis due to their tiny quantity (<5%) (Fig. S3). The formation of the large Au NAs was probably due to two strong interaction forces, *i.e.*, between DNA1 and cDNA1, and between -SH and Au in the DNA1-Au NPs and cDNA1-Au NPs.

3.3 Speculated self-assembly mechanism of the dsDNA-induced self-assembly strategy

Different from flexible ssDNA that could uncoil sufficiently to expose its positive bases in solution,²¹⁻²⁵ dsDNA was rigid and negatively charged, which was therefore difficult to flexibly bend and adsorb onto the surface of the negatively charged Au NPs through electrostatic attraction.^{26,27} Nevertheless, it was important to note that thiol groups had very strong affinity to metal NPs, which was utilized to assemble Ag NPs and effectively adjust particle spacing between Ag NPs.¹² The dsDNA presented here contained two thiol groups, which could form covalent bond with Au NPs. The strong interaction force of the Au-S covalent bond could perhaps make the dsDNA bend to some degree. In addition, the bithiol-modified dsDNA had a flexible alkyl chain (*i.e.*, -(CH₂)₆-) as a linker arm between its DNA bases and thiol group. Therefore, the strong Au-S bond and flexible -(CH₂)₆- alkyl chain enabled the dsDNA to partially bend and attach on the surface of the negatively charged Au NPs.

At relatively high Au NPs concentration (*i.e.*, the concentration ratio of Au NPs to dsDNA was 1:15 or higher), the bithiol-modified dsDNA easily absorbed onto the Au NPs surface

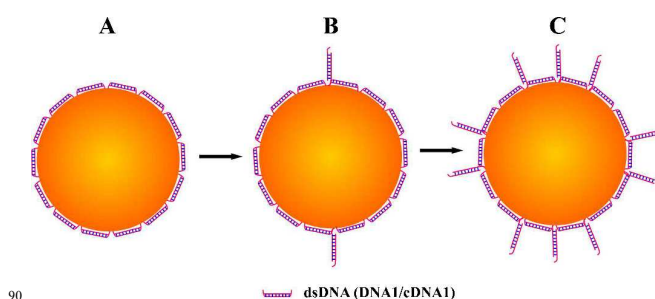


Fig. 4 Schematic representation of the Au NPs conjugated to the dsDNA at different concentration ratios.

through its strong affinity to the Au NPs (Fig. 4A). The adherence of dsDNA impeded the self-assembly of the Au NPs, which resulted in the appearance of only a single band. Increasing the dsDNA concentration, the dsDNA molecules would be saturated and even excessive on the surface of the Au NPs. The excessive dsDNA would erect up on the Au NPs surface, in which only a thiol group in the dsDNA could bond to the surface of the Au NPs due to steric hindrance (Fig. 4B). The erecting dsDNA was available and triggered the self-assembly of the Au NPs. For instance, when the concentration ratio of the Au NPs to dsDNA lowered to 1:20, the band began to separate (Lane 5 of Fig. 2), suggesting that the Au NPs began to assemble at this concentration ratio. Further lowering the concentration ratio to 1:40, the erecting dsDNA existed in all Au NPs (Fig. 4C) and thus the isolated Au NPs completely assemble into the Au NAs containing two, three, four, five or more Au NPs (Lanes 6 and 7 of Fig. 2).

3.4 Morphological images of the Au NAs assembled with two Au NPs

The different bands in Lanes 6 and 7 of Fig. 2 were cut out and extracted to obtain the different nanoassemblies, which were characterized by TEM, HRTEM, AFM and UV-vis absorption spectroscopy. The Au NAs obtained from the first band were conjugates of two Au NPs (Fig. 5A), which had a high yield (>88%, Fig. S4) far exceeding those of other self-assembly routes.^{15,28-30} The estimated gap value between the two in agreement with previous report.¹² However, the interparticle distance was far smaller than the theory value (*ca.* 13.8 nm), which may be due to the DNA bending in the dried dsDNA-Au NPs conjugates.²⁸ Fig. 5C gives a typical AFM image of the two-Au NAs prepared by the dsDNA self-assembly strategy. To avoid the NAs overlap, the AFM sample was prepared using extremely diluted solution of the dsDNA-Au conjugates. Scanning along

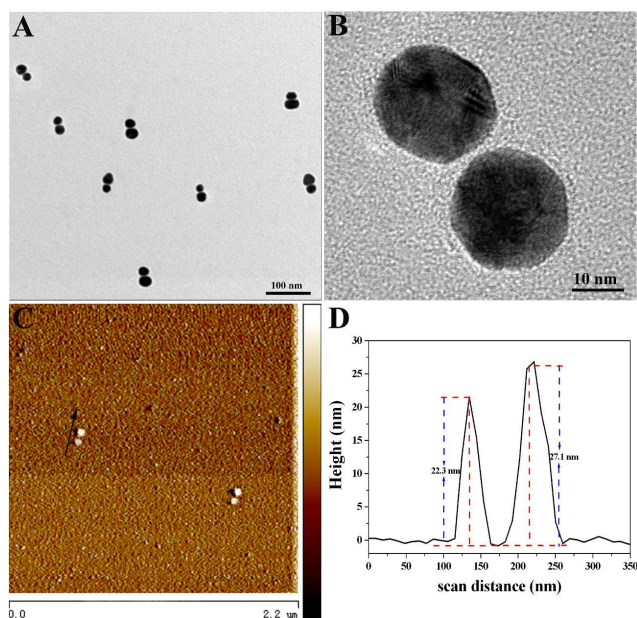


Fig. 5 (A) TEM, (B) HRTEM and (C) AFM images of the two-Au NPs NAs prepared by the dsDNA self-assembly strategy; (D) Scan-distance-dependence height plot of the two assembled Au NPs marked with an arrow in (C). The arrow in (C) is the linear scan direction.

assembled Au NPs was about 1.3 nm (Fig. 5B), which was nearly with the arrow's direction, there appeared two peaks corresponding two assembled Au NPs (Fig. 5D), the sizes of which were around 22.3 and 27.1 nm, respectively. The height (i.e., the assembled Au NP size) measurement was accurate because the sensitivity of AFM in height may be up to 1 nm, although the image of the X-Y plan was easily magnified and distorted in the course of AFM measurement.^{32,33}

3.5 TEM images of the Au NAs with 3-5 Au NPs

Fig. 6 gives typical TEM images of the Au NAs with three, four and five Au NPs that were also obtained by cutting out and extracting the second, third and fourth bands in the Lanes 6 and 7 of Fig. 2. It could be found that the Au trimers, tetramers and pentamers were successfully self-assembled by the dsDNA strategy, the yields of which were 80%, 76% and 67%, respectively. Of special emphasis here, the three-, four- and five-AuNPs NAs yields we obtained based on their corresponding TEM images (Fig. S5). To further verify the feasibility of bithiol-modified complementary dsDNA self-assembly strategy for large-sized Au NPs, assembling 48.0-nm Au NPs was performed. Fig. S6 gives TEM images of the 48.0-nm Au NPs and its two-, three- and four-AuNPs NAs prepared by the dsDNA self-assembly strategy. It could be clearly seen from Fig. S6 that the dsDNA strategy could be used to effectively assemble 48.0-nm Au NPs into its two-, three- and four-AuNPs NAs. Nevertheless, by comparison, the corresponding yields of the 48.0-nm Au NAs were lower than those of the 22.6-nm NAs. This could be contributed to its larger steric hindrance, which could perhaps be solved through increasing the length of the dsDNA chain. Therefore, it was feasible for the bithiol-modified complementary dsDNA strategy to assemble tunable size Au NPs in a large range through finely varying the dsDNA chain length.

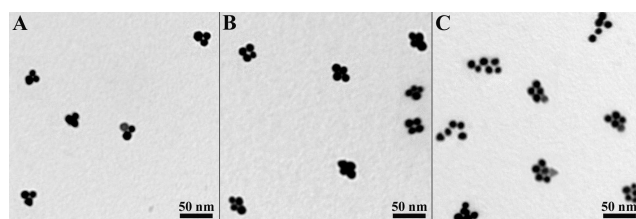


Fig. 6 TEM images of the (A) three-, (B) four- and (C) five-AuNPs NAs prepared by the dsDNA self-assembly strategy.

3.6 UV-vis spectra of the Au NPs and NAs solutions

UV-vis absorption spectroscopy is a powerful tool to fast and qualitatively monitor DNA-Au NPs self-assembly, relying on the fact that localized surface plasmon resonance (LSPR) properties depends sensitively on the assembled nanoparticle size,³⁴ shape³⁵ and size, shape and interparticle distance of assemblies.^{10,36,37} Fig. 7 shows UV-vis absorption spectra of the 22.6-nm Au NPs and NAs solutions. The Au NPs solution presented a sharp absorption peak at about 522 nm (Curve a), which was consistent with that theoretically calculated by Jain's group.³⁸ It was very interesting to note that the absorption peaks of the dsDNA-induced nanoassemblies displayed a red-shift and broadening when the Au NPs assembled and its assembled Au NPs numbers increased (Curves b-e).

The absorption peak of the two-AuNPs NAs red-shifted to

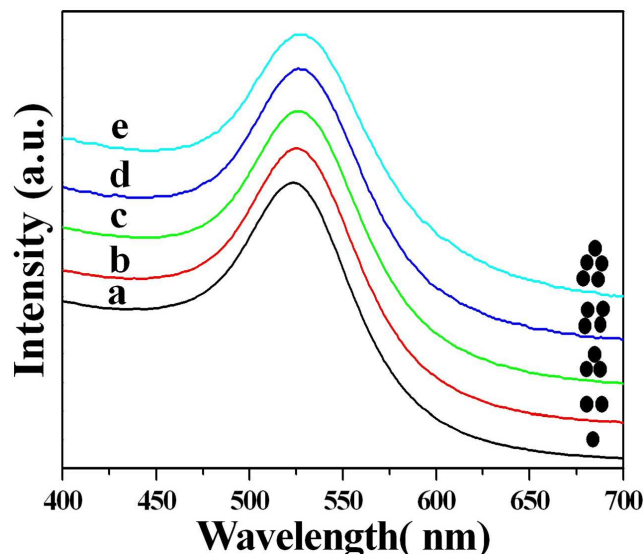


Fig. 7 UV-vis absorption spectra of (a) Au NPs solution and (b) two-, (c) three-, (d) four- and (e) five-AuNPs NAs solutions prepared by the dsDNA self-assembly strategy.

around 525 nm and was very narrow (Curve b), indicating that the Au NPs overwhelmingly assembled into Au dimers. When three Au NPs were employed to assemble, there still appeared a narrow peak and the peak had only a slightly red-shift from *ca.* 522 to 527 nm (Curve c). This suggested that the triangular (not linear) assemblies were the main product of the three-AuNPs NAs because linear Au NAs would have perhaps two absorption peaks (*i.e.*, transverse and longitude absorption peaks) or more red-shift. Also, the absorption peak (approximately 529 nm) of the four-AuNPs NAs had also only a slight red-shift (Curve d), revealing that the four Au NPs mainly assembled into quadrangle shape. Nevertheless, when the five Au NPs were utilized to assemble by the dsDNA linkers, its SPR absorption, besides a small red-shift, had a relatively broad peak (Curve e), which could be possibly contributed to its relatively low yield.

4 Conclusions

In summary, we have demonstrated a simple and effective strategy for the directed and high-yield assembly of large-sized Au NPs through using the bithiol-modified dsDNA architectures. Compared with traditional methods, our strategy did not require the preparation and electrophoresis separation of the conjugate between Au NPs and ssDNA and avoided the lengthening and melting of additional long chain DNA. Moreover, the preliminary study showed that the bithiol-modified dsDNA architectures played an important role in the high-yield self-assembly of the large-sized Au NPs. Therefore, this straightforward and high efficiency methodology opens a new avenue of DNA-induced self-assembly of large-sized metal NPs.

Acknowledgements

We are grateful to the National Natural Science Foundation of China (Grants 21173087 and 51273070).

Notes and references

- ^a Analytical and Testing Center, Jinan University, Guangzhou 510632, China. E-mail: yuxiang@jnu.edu.cn
- ^b Key Lab of Fuel Cell Technology of Guangdong Province, Department of Chemistry, College of Chemistry and Chemical Engineering, South China University of Technology, Guangzhou 510640, China. Fax & Tel: +86 20 2223 6670; E-mail: jghusc@scut.edu.cn; jyliu@scut.edu.cn
- ^c Guangzhou Center for Disease Control and Prevention, Guangzhou 510440, China.
- [#] Yanfang Cheng and Guiping Yu contributed equally to this work.
- [†] Electronic Supplementary Information (ESI) available: TEM image of the Au NPs prepared by the citrate reduction route, TEM image of the conjugates prepared at the 1:15 concentration ratio of Au NPs to dsDNA, Gel electropherogram of the Au NPs and large Au NAs prepared by stepwise assembly, TEM of the two-Au NPs NAs prepared by the dsDNA self-assembly strategy, Large scale TEM images of the Au NAs with three, four and five 22.6-nm Au NPs and TEM images of the 48.0-nm Au NPs and its two-, three- and four-AuNPs NAs prepared by the dsDNA self-assembly strategy. See DOI: 10.1039/b000000x/
- S. J. Tan, M. J. Campolongo, D. Luo and W. L. Cheng, *Nat. Nanotechnol.*, 2011, **6**, 268-276.
 - W. L. Cheng, M. J. Campolongo, J. J. Cha, S. J. Tan, C. C. Umbach, D. A. Muller and D. Luo, *Nat. Mater.*, 2009, **8**, 519-525.
 - H. Yan, S. H. Park, G. Finkelstein, J. H. Reif and T. H. LaBean, *Science*, 2003, **301**, 1882-1884.
 - A. M. Hung, H. Noh and J. N. Cha, *Nanoscale*, 2010, **2**, 2530-2537.
 - L. Piantanida, D. Naumenko and M. Lazzarino, *RSC Adv.*, 2014, **4**, 15281-15287.
 - A. Kuzyk, R. Schreiber, Z. Y. Fan, G. Pardatscher, E. M. Roller, A. Hogege, F. C. Simmel, A. O. Govorov and T. Liedl, *Nature*, 2012, **483**, 311-314.
 - Y. H. Zheng, T. Thai, P. Reineck, L. Qiu, Y. M. Guo and U. Bach, *Adv. Funct. Mater.*, 2013, **23**, 1519-1526.
 - N. Guarrotxena, Y. Ren and A. Mikhailovsky, *Langmuir*, 2011, **27**, 347-351.
 - Y. F. Cheng, X. D. Lai, Y. Yan, J. Y. Peng, X. Yu, C. Ye, C. L. Fu, J. Y. Liu, Y. X. Chen and J. Q. Hu, *RSC Adv.*, 2013, **3**, 19942-19945.
 - X. M. Feng, F. X. Ruan, R. J. Hong, J. S. Ye, J. Q. Hu, G. Q. Hu and Z. L. Yang, *Langmuir*, 2011, **27**, 2204 - 2210.
 - Y. Ohya, N. Miyoshi, M. Hashizume, T. Takuya, T. Uehara, S. Shingubara and A. Kuzuya, *Small*, 2012, **8**, 2335-2340.
 - D. Zanchet, C. M. Micheel, W. J. Parak, D. Gerion and A. P. Alivisatos, *Nano Lett.*, 2001, **1**, 32-35.
 - J. W. Kim, J. H. Kim and R. Deaton, *Angew. Chem. Int. Ed.*, 2011, **50**, 9185-9190.
 - S. Bidault, F. J. G. de Abajo and A. Polman, *J. Am. Chem. Soc.*, 2008, **130**, 2750-2751.
 - M. P. Busson, B. Rolly and B. Stout, *Nano Lett.*, 2011, **11**, 5060-5065.
 - Y. J. Huang and D. H. Kim, *Langmuir*, 2011, **27**, 13861-13867.
 - L. G. Xu, H. Kuang, C. L. Xu, W. Ma, L. B. Wang and N. A. Kotov, *J. Am. Chem. Soc.*, 2012, **134**, 1699-1709.
 - X. Lan, Z. Chen, B. Liu, B. Ren, J. Henzie and Q. B. Wang, *Small*, 2013, **13**, 2308-2315.
 - S. J. Hurst, A. K. R. Lytton-Jean and C. A. Mirkin, *Anal. Chem.*, 2006, **78**, 8313-8318.
 - G. Chen, Y. Wang, L. H. Tan, M. Yang, L. S. Tan, Y. Chen and H. Chen, *J. Am. Chem. Soc.*, 2009, **131**, 4218-4219.
 - H. X. Li and L. J. Rothberg, *Anal. Chem.*, 2004, **76**, 5414-5417.
 - H. Wei, B. L. Li, J. Li, E. K. Wang and S. J. Dong, *Chem. Commun.*, 2007, **36**, 3735-3737.
 - L. H. Wang, X. F. Liu, X. F. Hu, S. P. Song and C. H. Fan, *Chem. Commun.*, 2006, **36**, 3780-3782.
 - Z. D. Wang, J. H. Lee and Y. Lu, *Adv. Mater.*, 2008, **20**, 3263-3267.
 - J. Zhang, L. H. Wang, D. Pan, S. P. Song, F. Y. C. Boey, H. Zhang and C. H. Fan, *Small*, 2008, **4**, 1196-1200.
 - H. X. Li and L. J. Rothberg, *J. Am. Chem. Soc.*, 2004, **126**, 10958-10961.
 - H. X. Li and L. J. Rothberg, *P. Nat. Acad. Sci. USA*, 2004, **101**, 14036-14039.
 - J. Y. Choi, Y. T. Kim and T. S. Seo, *ACS Nano*, 2013, **7**, 2627-2633.

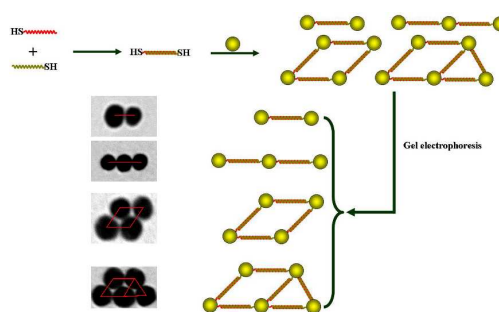
- 29 T. Zhang, P. Chen, Y. W. Sun, Y. Z. Xing, Y. Yang, Y. C. Dong, L. J. Xu, Z. Q. Yang and D. S. Liu, *Chem Commun.*, 2011, **47**, 5774-5776.
- 30 H. Yao, C. Q. Yi, C. H. Tzang, J. J. Zhu and M. S. Yang, *Nanotechnology*, 2007, **18**, 015102-015108.
- 5 31 S. A. Claridge, A. J. Mastroianni, Y. B. Au, H. W. Liang, C. M. Micheel, J. M. J. Fréchet and A. P. Alivisatos, *J. Am. Chem. Soc.*, 2008, **130**, 9598-9605.
- 32 P. M. Kosaka, S. González, C. M. Domínguez, A. Cebollada, A. S. Paulo, M. Calleja and J. Tamayo, *Nanoscale*, 2013, **5**, 7425-7432.
- 10 33 J. Q. Hu, Y. Zhang, B. Liu, J. X. Liu, Y. F. Xu, Y. X. Jiang, Z. L. Yang and Z. Q. Tian, *J. Am. Chem. Soc.*, 2004, **126**, 9470-9471.
- 34 N. Borovok, E. Gillon and A. Kotlyar, *Bioconjugate Chem.*, 2012, **23**, 916-922.
- 15 35 L.V. Brown, H. Sobhani, J. B. Lassiter, P. Nordlander and N. J. Halas, *ACS Nano*, 2010, **4**, 819-832.
- 36 A. Tao, P. Sinsersuksakul and P. D. Yang, *Angew. Chem. Int. Ed.*, 2006, **45**, 4597-4601.
- 37 K. C. Woo, L. Shao, H. J. Chen, Y. Liang, J. F. Wang and H. Q. Lin, *ACS Nano*, 2011, **5**, 5976-5986.
- 20 38 P. K. Jain, K. S. Lee, I. H. El-Sayed and M. A. El-Sayed, *J. Phys. Chem. B*, 2006, **110**, 7238-7248.

Table of contents

A simple and effective strategy for the directed and high-yield assembly of large-sized gold nanoparticles driven by bithiol-modified complementary dsDNA architectures

Yan-Fang Cheng, Gui-Ping Yu, Yuan Yan, Jian-Yu Liu,* Cui Ye, Xiang Yu,* Xuan-Di Lai and Jian-Qiang Hu*

A simple and effective strategy for the directed and high-yield assembly of large-sized Au NPs was demonstrated by bithiol-modified dsDNA.



Graphical Abstract

A simple and effective strategy for the directed and high-yield assembly of large-sized Au NPs has been demonstrated by bithiol-modified complementary dsDNA architectures. Compared with traditional methods, this strategy enabled excellent self-assembly of large-sized Au NPs, while obviating the conjugate of Au NPs to ssDNA and the use of long chain DNA.

